International Journal of
Science and Engineering Investigations vol. 8, issue 92, September 2019
Received on September 3, 2019 ISSN: 2251-8843

Numerical Investigation of Improving Turbulent Heat Transfer in the Separated and Reattached Flow Regions Downstream of a Downward-Facing Step Using Vortex Generators

M. Mohammadi[1], S. Madanshenas[2], M. Oreijah[3], M. H. Mohamed[3]
[1]Faculty of Engineering, Mechanical Engineering Department, Urmia University, Urmia, Iran
[2]Department of Mechanical Engineering, Tabriz Branch, Islamic Azad University, Tabriz, Iran
[3]Mechanical Engineering Dept., College of Engineering and Islamic Architecture, Umm Al-Qura University, P.O. 5555, Makkah, Saudia Arabia
[4]Renewable Energy Lab. Faculty of Engineering-Mattaria, Helwan University, Cairo, Egypt
([1]m.mohammadi67@gmail.com)

Abstract-Numerical ascertainment of improving turbulent heat transfer in the separated and reattached flow regions downstream of a downward-facing step is investigated by means of three-dimensional flow predictions executed in ANSYS FLUENT. Since pressure loss adversely affects the performance, main objective of present study is to maximize heat transfer (mean Stanton number) while minimizing pressure loss through the channel. In order to simplify comparison process, the model represented in a related paper with Reynolds number of 26000 (based on step height and upstream undisturbed velocity) is simulated and results are compared with experimental data. Three shapes of vortex generators (quadrant, isosceles triangle and square) each one in two sizes are then added and have been used to agitate the flow and affect turbulent heat transfer. The best performance is achieved by the large isosceles triangle. It results in highest increasing of area weighted average surface Stanton number by the pressure loss. Then, this model with the highest performance has been moved along the channel and its best position is probed and found to be near step. Best shape with best position's performance is then investigated for a wide range of Reynolds number. The results indicate that increasing Reynolds number adversely affects the performance.

Keywords- *Vortex Generator, CFD, Separated and Reattached Flow Regions, Turbulent Heat Transfer, Stanton Number, Downward-Facing Step*

I. INTRODUCTION

Turbine blades and electronic devices' cooling, flow around aircraft, hills and buildings, combustion chamber and some earth science applications are examples of technologically important phenomenon called flow separation and reattachment. In order to optimally enrich the heat transfer rate in such applications, the separated and reattached regions shall be effectively controlled. Even though the geometry of downward-facing step problem is simple, the resulting structure of the flow field is sophisticated and has been subject of numerous works done by experienced investigators [1-18]. For heat transfer cases, separation and reattachment results in substantial growth in heat transfer rates and huge alteration in heat transfer coefficient [14]. In this regard, Kumar et al. [1] studied the control of laminar fluid flow and heat transfer characteristics over a backward facing step. By two-dimensional numerical simulation, the fin's geometrical parameter effects for two different Reynolds numbers have been investigated. According to Kumar et al. [1], placing a fin at the step is the most critical case and a little movement in upstream direction may generate thorough transformation in flow and thermal behavior. Atashafrooz [2] performed three-dimensional simulation of nanofluid flow over inclined step. He found out that increasing the nanoparticles volume fraction results in considerable increase in the reattachment length of the recirculation zone. Xu et al. [4] have studied the fluid flow and heat transfer characteristics of backward-facing step for low and middle range Reynolds number. According to Xu et al. [4], Re = 1000 leads to highest value for the time averaged reattachment length. In addition, this length is decreased as the Reynolds number is increased. In another attempt, Kumar et al. [5] have studied the fluid flow and heat transfer characteristics of an oscillating fin mounted on the top wall of backward facing step. They concluded that oscillating fin represents a more promising performance in comparison with different types of stationary fin arrangement. Tsay et al. [6] numerically studied the effects of the dimensionless baffle height, thickness, and distance between the backward-facing step and baffle on the flow structure and heat transfer characteristics. They found out that the baffle width is not an important parameter on heat transfer. Heshmati et al. [7] performed a numerical simulation and used nanofluids for laminar mixed convective flows over backward facing steps. They reported that 4% nanoparticle volume fraction and 20 nm nanoparticle

diameter resulted in greatest heat transfer enhancement. Nie et al. [8] used three-dimensional numerical simulations in order to study the effects of baffle on flow adjacent to backward-facing step in a rectangular duct. They reported that setting up of a baffle on the upper wall improves the heat transfer. Abrous et al. [9] studied backward-facing step and concluded that Reynolds-averaged turbulence modeling is predominantly unable to prognosticate the fluid dynamics and heat transfer accurately. Avancha et al. [10] used a coupled, compressible, finite-volume code to model heat transfer of downstream of a backward-facing step using Large-eddy simulation and focused mostly on flows in which properties were varied considerably by heat transfer. A similar work with Large-eddy simulation was done by Labbe et al. [14] in which a subgrid-scale model with a constant subgrid-scale Prandtl number was used for simulation. They validated their simulations by a comparison with mean reattachment length with empirical data. However, they reported maximum heat transfer to occur at the point of reattachment, in contrary with both Large-eddy simulation of Avancha [10] and experimental data of Vogel [20]. It is hard to judge because of lack of experimental data, and it is unclear why this occurred in these simulations. Wang et al. [21] employed large eddy method and Lagrangian techniques to simulate the turbulent flow over a backward-facing step. This investigation revealed that the particles follow a path when the vorticity of the gas phase is slight. The step height effects on separation and reattachment for convective flow adjoining a backward-facing step was investigated by Nie et al. [15]. Feng et al. [12] conducted an experimental research to visualize the turbulent separated flow and measure the wall pressure over a backward-facing step. The results showed that the negative peak of the time varying wall pressure was in phase with the passage of the local large scale vertical structure beneath the separation bubble and the reattachment zone.

Yoshikawa et al. [22] performed an experimental investigation on effects of step height on turbulent heat transfer around downward-facing step. Different step heights were examined and surface Stanton number for each one was reported.

In current study, these cases are simulated by computational fluid dynamics and first height is chosen as the primary shape. Some baffles are set and their effects on turbulent heat transfer are investigated. Along with increased heat transfer, these baffles cause pressure loss which is believed to be the most important repercussion and needs to be scrutinized. So, the benefit-cost ratio (B.C.R) is defined as increasing Stanton number by decreasing pressure loss to make a more efficacious assessment index feasible. Assuming the pressure loss of the channel without baffle (considered as the primary shape) to be ΔPint, the heated wall's area weighted average surface Stanton number to be Stint, pressure loss of flow through channel after adding baffle to be ΔPbaf and the heated wall's area weighted average surface Stanton number to be Stbaf, the benefit-cost ratio could be formulated as:

$$\text{B.C.R} = \frac{\frac{(\text{St baf} - \text{St int})}{\text{Stint}}}{\frac{(\Delta\text{P baf} - \Delta\text{P int})}{\Delta\text{P int}}} \quad (1)$$

As mentioned above, most researches were conducted on effects of step's size, height and number or different turbulence models' accuracy on prognosticating separation and reattachment regions. In current investigation, different shapes of vortex generators with different sizes and at different locations and with different Reynolds numbers will be implemented and their effects on turbulent heat transfer will be studied. These obstacles increase maximum Stanton number near step, caused by vortices and sometimes improve it in latter parts of channel.

II. NUMERICAL METHODOLOGY

A. Geometry description

Figure 1 depicts the geometry considered in this simulation. As discussed thoroughly by Yoshikawa et al. [22], just the lower downstream wall was heated by constant heat flux while keeping all other walls isolated and being exposed to air flow stream with undisturbed velocity of 20 m/s. In this figure, W_1 represents the entrance height and varies from 0.08 m to 0.28 m along with step height H and exit height W_2, while maintaining width constant at 0.2 m. Stanton number is reported for each case. Since correctly simulating one case is sufficient for validation progress, first case with configuration presented in table 1 is drawn and its flow field is solved.

TABLE I. GEOMETRY AND IMPORTANT PARAMETERS

Channel length X_t (m)	Total height W_2 (m)	Entrance height W_1 (m)	Step height H (m)	Step length X_E (m)	Heat transfer rate q_w (w/m^2)	Free stream velocity U_{ref} (m/s)	Depth W (m)
1	0.1	0.08	0.02	0.2	1000	20	0.2

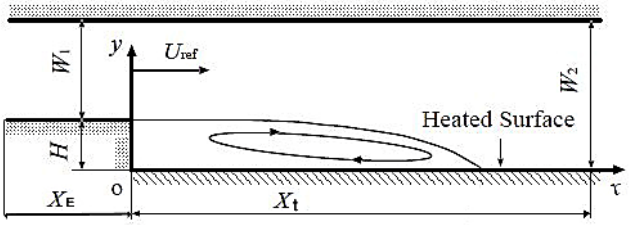

Figure 1. Geometry and boundary conditions [22]

B. Governing equations

Continuity, energy and momentum conservation equations are the main governing equations would be shown in three-dimensions as:

$$\frac{\partial u}{\partial x} + \frac{\partial \upsilon}{\partial y} + \frac{\partial \omega}{\partial z} = 0 \quad (2)$$

$$u\frac{\partial r}{\partial x}+\upsilon\frac{\partial r}{\partial y}+\omega\frac{\partial r}{\partial z}=-\frac{1}{\rho}\frac{\partial p}{\partial y}+\alpha(\frac{\partial^2 r}{\partial x^2}+\frac{\partial^2 r}{\partial y^2}+\frac{\partial^2 r}{\partial z^2}) \quad (3)$$

$$u\frac{\partial u}{\partial x}+\upsilon\frac{\partial u}{\partial y}+\omega\frac{\partial u}{\partial z}=-\frac{1}{\rho}\frac{\partial p}{\partial x}+\alpha(\frac{\partial^2 u}{\partial x^2}+\frac{\partial^2 u}{\partial y^2}+\frac{\partial^2 u}{\partial z^2}) \quad (4)$$

$$u\frac{\partial \upsilon}{\partial x}+\upsilon\frac{\partial \upsilon}{\partial y}+\omega\frac{\partial \upsilon}{\partial z}=-\frac{1}{\rho}\frac{\partial p}{\partial y}+\upsilon(\frac{\partial^2 \upsilon}{\partial x^2}+\frac{\partial^2 \upsilon}{\partial y^2}+\frac{\partial^2 \upsilon}{\partial z^2}) \quad (5)$$

$$u\frac{\partial \omega}{\partial x}+\upsilon\frac{\partial \omega}{\partial y}+\omega\frac{\partial \omega}{\partial z}=-\frac{1}{\rho}\frac{\partial p}{\partial z}+\upsilon(\frac{\partial^2 \omega}{\partial x^2}+\frac{\partial^2 \omega}{\partial y^2}+\frac{\partial^2 \omega}{\partial z^2}) \quad (6)$$

Yilmaz et al. [23] reported the Realizable K-ε turbulence model to be capable of properly simulating these models. So, Realizable K-ε model of transport equations with enhanced wall treatment is set to calculate the turbulence kinetic energy K and dissipation rate ε as:

$$\frac{\partial}{\partial x}(\rho k u)=\frac{\partial}{dy}\left(\left[\left(\mu+\frac{\mu_t}{\sigma_\varepsilon}\right)\frac{\partial k}{\partial y}\right]\right)+G_k-\rho\omega \quad (7)$$

$$\frac{\partial}{\partial x}(\rho\varepsilon u)=\frac{\partial}{dy}\left(\left[\left(\mu+\frac{\mu_t}{\sigma_\varepsilon}\right)\frac{\partial \varepsilon}{\partial y}\right]\right)+C_{1\varepsilon}\frac{\varepsilon}{k}(G_K+C_{3\varepsilon}G_b)-C_{2\varepsilon}\rho\frac{\varepsilon^2}{K} \quad (8)$$

where G_k is computed by [19]:

$$G_K=-\rho\overline{v'u}\frac{\partial v}{\partial x} \quad (9)$$

and μ_t is calculated by:

$$\mu_t=\rho C_P\frac{k^2}{\varepsilon} \quad (10)$$

The values used for constants are shown in table 2 [19].

TABLE II. CONSTANTS OF THE TRANSPORT EQUATIONS

C1ε	C2ε	C3ε	σk	σε
1.44	1.92	0.09	1.0	1.3

C. Numerical model validation

All the governing equations along with the boundary conditions are solved by Ansys-Fluent 17.2. Standard atmospheric values at sea level with constant temperature is set for air properties as operating fluid. Steady state condition is presumed and pressure based is used to relate the momentum and mass conservation equations. Second order upwind scheme is used to solve the convective terms in the momentum and energy equations and velocity-pressure coupling is done by SIMPLE algorithm. Velocity inlet boundary condition is set for fluid entrance, all walls except heated wall (figure 1) are insulated and outlet is set as right side's boundary condition.

Yoshikawa et al. [22] reported performance as heated wall surface Stanton number and same pattern is used here to evaluate simulation process. The discretization has been performed and computational domain has been divided into quadrilateral elements using MultiZone method, so that the best results would be achieved after adding baffles. According to Yoshikawa et al. [22], heated wall's area weighted average Stanton number should be 0.003376 and reach maximum amount at almost 0.11 m after step. Figure 2 displays the result of increasing element numbers in order to achieve mesh independency.

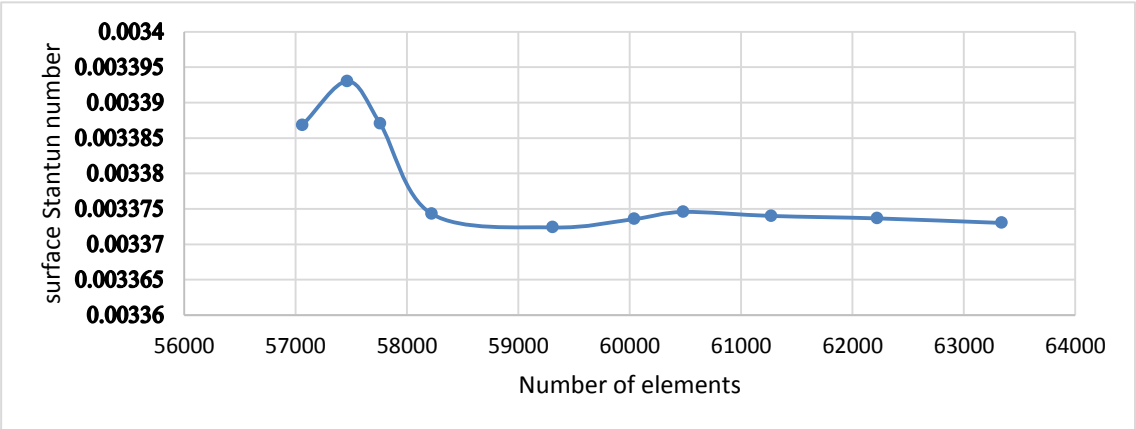

Figure 2. Mesh independence study

In order to optimally predict the boundary layer effects, an inflation with 18 layers is set on downstream wall, assigning 4 x 10^{-4} m for the first layer thickness and 1.18 as growth rate.

Figure 2 implies that the case with 60,480 elements displays best performance and highest likeness with experimental results.It also depicts that the results are diverged by increasing elements, which can be a result of round-off errors. So, previous case with 60,480 elements, 12 layers as inflation, minimum layer thickness of 2 x 10^{-4} m and growth rate of 1.15 is set as primary case and shown in figure 3. It also ensures achieving the constraint of $y+ \leq 5$.

As shown in figure 3, a finer mesh is set near the walls of the channel especially in the vicinity of step so that high gradients in thermal and hydrodynamic boundary layer and recirculation region downstream of the step could be resolved in best manner. Exerting previously discussed boundary conditions on discretized domain and applying Realizable K-ε turbulence model with Enhanced Wall Functions would lead to an acceptable agreement between experimental and numerical results, as shown in figure 4. Stanton number is used to measure the ratio of heat transferred to a fluid to the thermal capacity of fluid and is defined as:

$$St = \frac{Nu}{Re\ Pr} \tag{11}$$

Figure 4 represents a good agreement between experimental and numerical results and so, it can be concluded that this simulation can basically study the effects of different baffles. Numerical investigation reveals heated wall's surface Stanton number to be St_{int} = 0.0033745618 and pressure loss to be ΔP_{int} = 174.14288 Pa. So, these are set as primary values. Consequently, these values will be used in order to evaluate each baffle's performance.

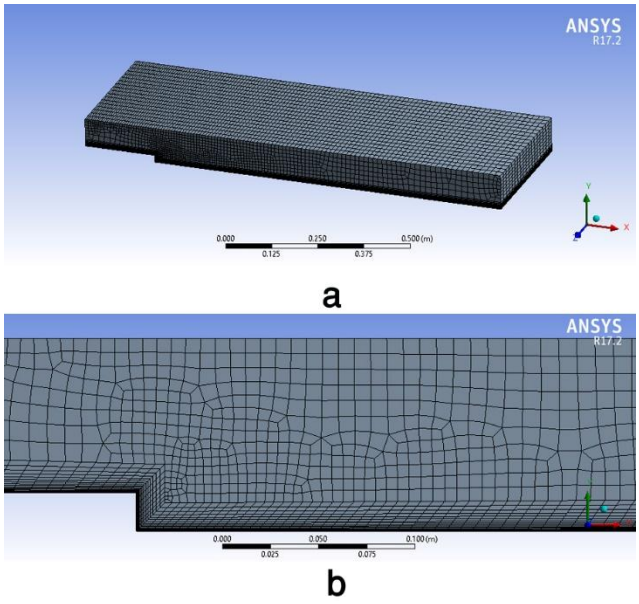

Figure 3. Domain mesh a) entire domain b) mesh in the vicinity of step

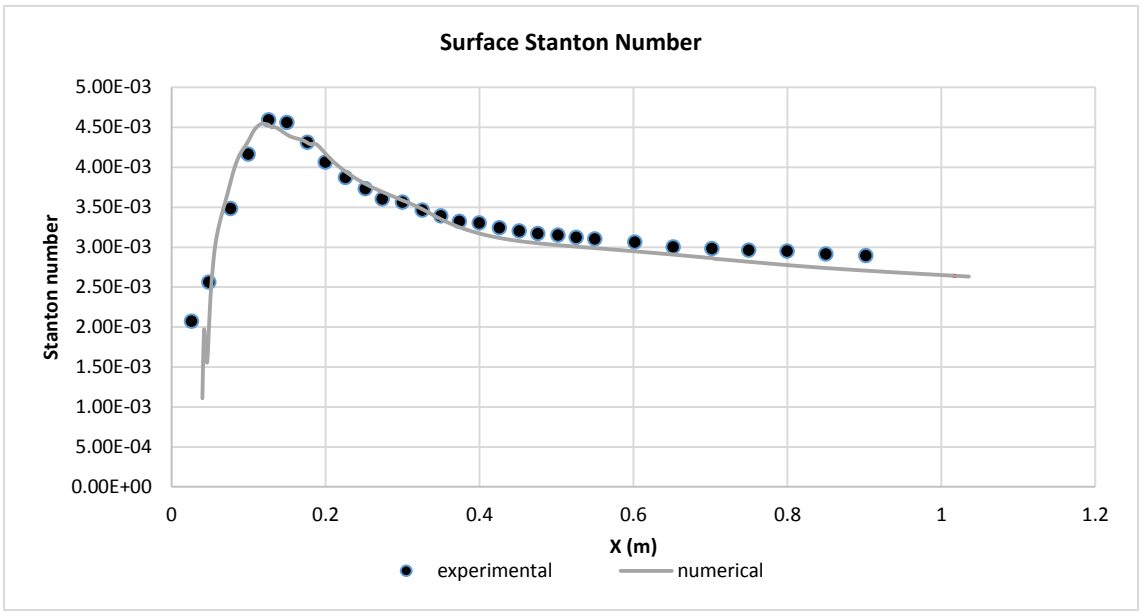

Figure 4. Comparison between experimental and numerical surface Stanton number

III. RESULTS AND DISCUSSION

Quadrant, square and triangle are three forms of baffles which will be studied in this section, each one in small and large sizes and with 0.005 m distance from the step, as depicted in figure 5. Increasing heat transfer rate and thus Stanton number is anticipated because of created agitation in fluid regime caused by the baffle. As mentioned above, this agitation increases pressure loss along with increasing Stanton number. To encounter this problem effectively and make a practical comparison feasible, the relative rising in heated wall's area weighted average surface Stanton number by relative increase in pressure loss is defined as benefit-cost ratio (B.C.R) (equation 1) and stands for the system's efficiency. Investigation continues with choosing the case with highest performance and moving its obstacle along the wall to study baffle's position effects and same process is repeated again. Research ends with determining the effects of fluid velocity (Reynolds number) on performance.

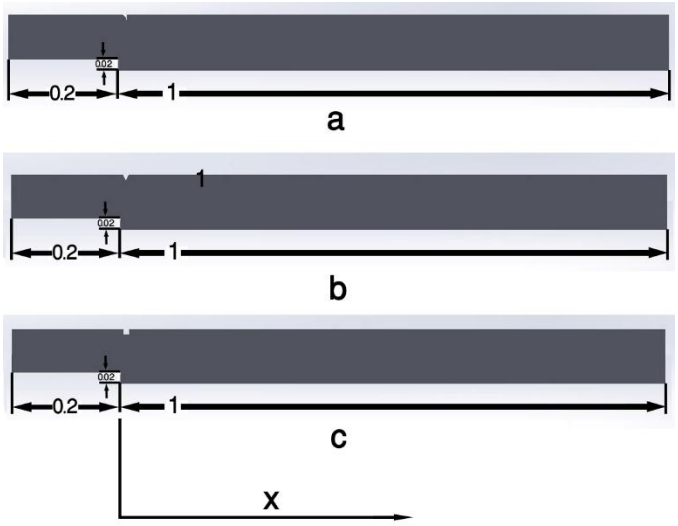

Figure 5. Baffles' types a) quadrant b) triangle c) square

A. *Baffle's shape and size*

First step in this study is to determine the best obstacle form and its proper size. As discussed above, three forms each one in two sizes are proposed for this section and will be studied in next section.

1) *Small quadrant*

First obstacle to be studied is a quadrant with 0.01 m radius and 0.005 m horizontal distance from the step, as shown in figure 6. Domain meshing is just like the primitive case while 12 layers of inflation quadrilateral mesh is used for meshing the baffle. Setting same boundary conditions and solving computational domain reveals that the heated wall's surface Stanton number will increase 3.25% while 16.93% rise in pressure loss is anticipated. As a consequence, B.C.R is going be 0.1919. As depicted in figure 6, adding small quadrant affects the flow regime and makes the maximum Stanton number increase, augmentation in performance is due to higher convection heat transfer coefficient at the separating and reattaching region. Adding baffle causes the flow regime to be more agitated and formed vortices to be invigorated, which would lead to a noticeable increase in separating and reattaching region. Because of its position and small size, this baffle cannot profoundly affect the downstream flow and surface Stanton number has almost the same behavior as primary case. Stream function at the middle is also shown in figure 6 to make these discussions more tangible.

2) *Large quadrant*

Second case covered in this section is a larger quadrant with 0.02 m radius and same position as previous baffle, 0.005 m horizontal distance from the step, as shown in figure 7. Boundary conditions and domain meshing are held identical, and baffle is again meshed with 12 layers of inflation quadrilateral mesh. Solving computational domain unveiled the amplification in heated wall surface Stanton number by this baffle to be 22.03% while 43.13% more pressure loss has taken place. Thus, the benefit-cost ratio equals 0.5108. Baffle's shape and position, heated wall surface Stanton number after adding large quadrant baffle in comparison with primary case and stream function are depicted in figure 7. Obviously, larger quadrant affects heat transfer process more significantly and makes both maximum Stanton number and area weighted average surface Stanton number to be higher in comparison with the small quadrant. Unlike previous case, it can also increase heat transfer downstream of the channel, because of its size and the fact that it manipulates flow regime more profoundly, making it more turbulent and increasing convection heat transfer coefficient. However, this leads to higher pressure loss and consequently lower B.C.R.

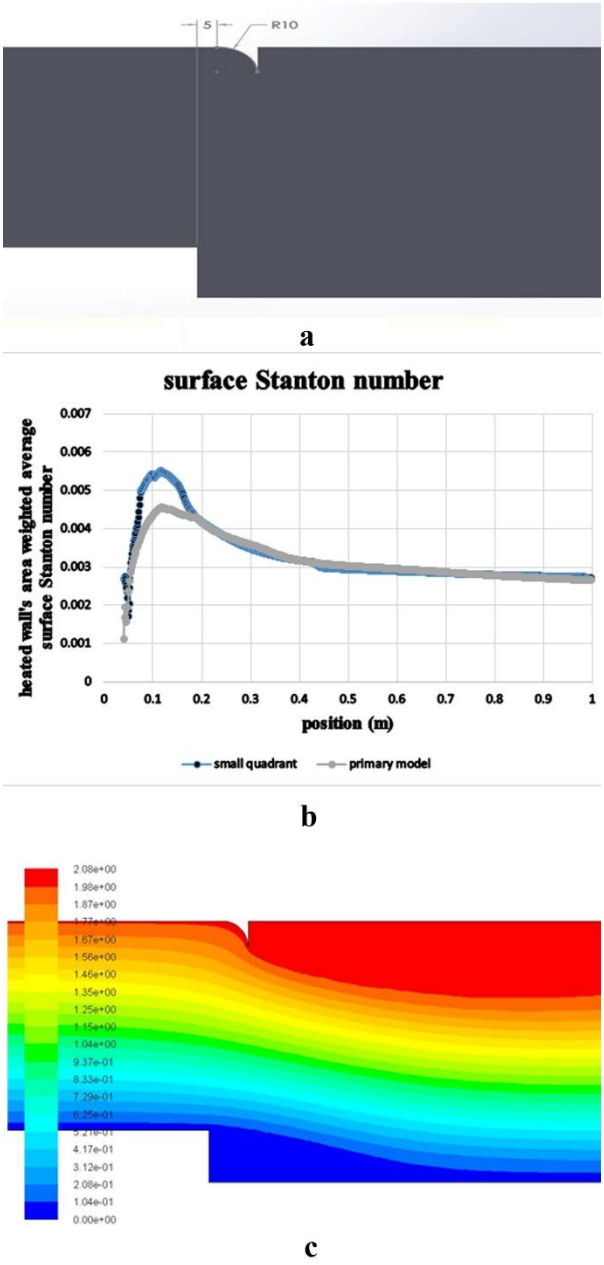

Figure 6. a)Baffle's shape and position (mm), b) Surface Stanton number, c) Stream function

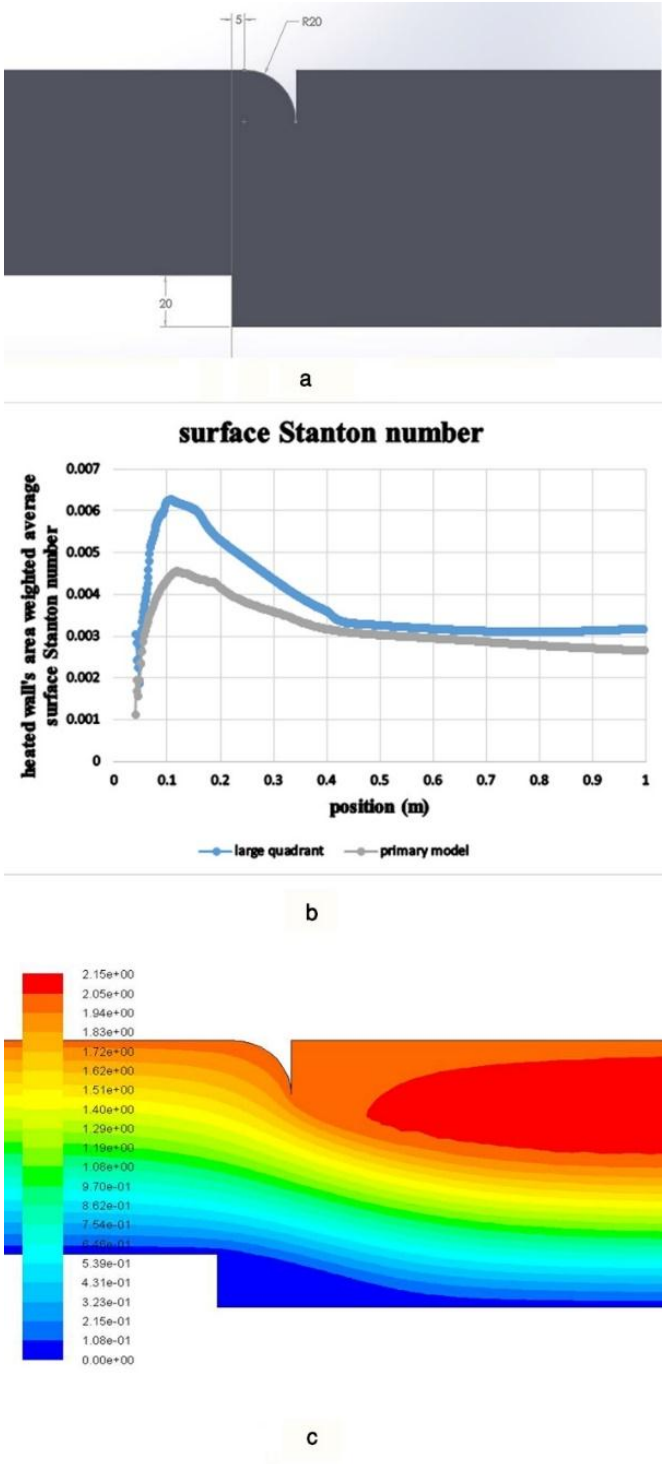

Figure 7. a) Baffle's shape and position (mm), b) Surface Stanton number, c) Stream function

a) Small isosceles triangle

Next form to be studied is an isosceles triangle with equal base and height of 0.01 m and just like previous baffles, has 0.005 m horizontal distance from the step as displayed in figure 8. Setting same domain mesh and boundary conditions as former cases which have been studied so far and solving the computational domain represents that installing this baffle will rise the heated wall's area weighted average Stanton number by 2.155% while 16.125% more pressure drop is observed, thus the B.C.R will be 0.1337. Along with baffle's shape and position, heated wall surface Stanton number before and after adding isosceles triangle and stream function are depicted in figure 8. Due to its small size, this baffle performs like the small quadrant and just increases maximum Stanton number, unable to impressively affect downstream flow. Fortifying generated vortices in separated and reattached region results in a slight improvement in heat transfer and consequently, scant pressure loss is detected.

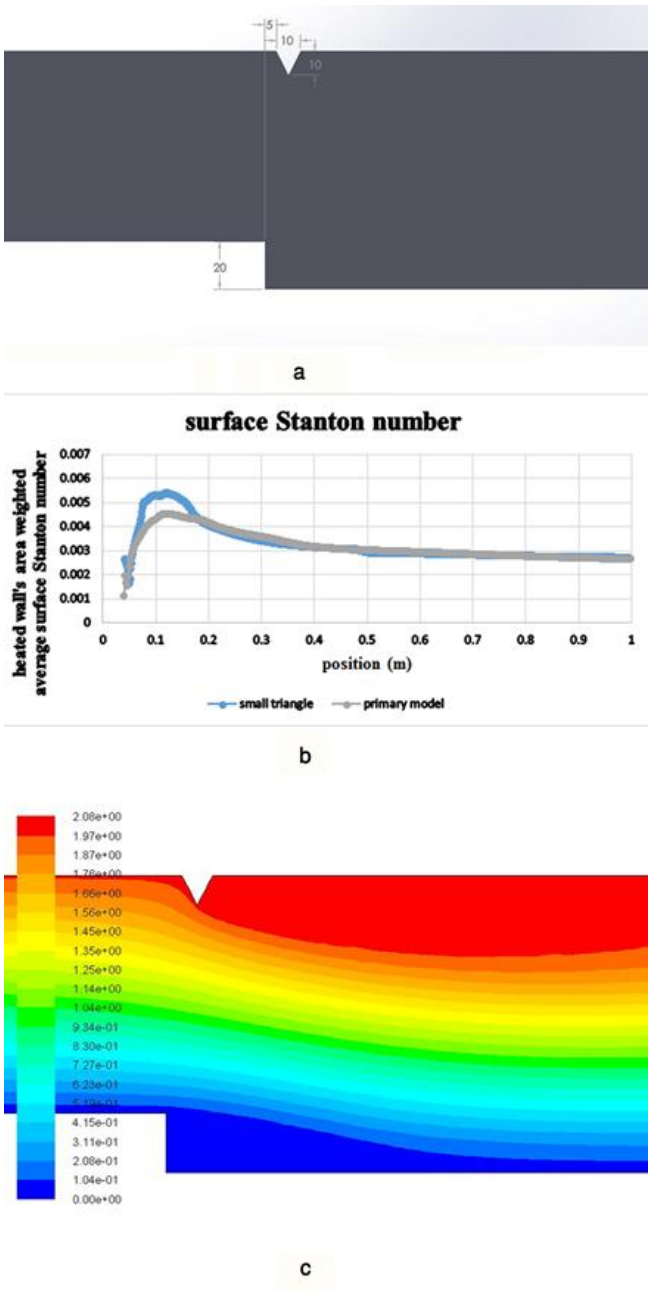

Figure 8. a) Baffle's shape and position (mm), b) Surface Stanton number, c) Stream function

b) Large isosceles triangle

Larger isosceles triangle with equal base and height of 0.02 m and same position as previous cases, 0.005 m horizontal distance from the step, as shown in figure 9 is the fourth model to be studied. This triangle has replaced previous one and consequently, has the same boundary conditions and domain mesh with 12 layers inflation quadrilateral mesh around the triangle. Studies revealed that this baffle increased surface area weighted average Stanton number by 27.598% and rose pressure drop by 43.142%, resulting in 0.6397 B.C.R. Just like previous models, the shape and position of this baffle, heated wall surface Stanton number in comparison with primary case and stream function are depicted in figure 9. Isosceles triangle displayed a similar manner with quadrant in effect of size. Larger size with same form improved the heat transfer more conspicuously. Heated wall's surface Stanton number downstream of the channel has been improved along with a considerable growth in separating and reattachment region caused by generated vortices and turbulent flow. Higher Stanton number caused by baffle is adversely affected by comparatively high pressure loss.

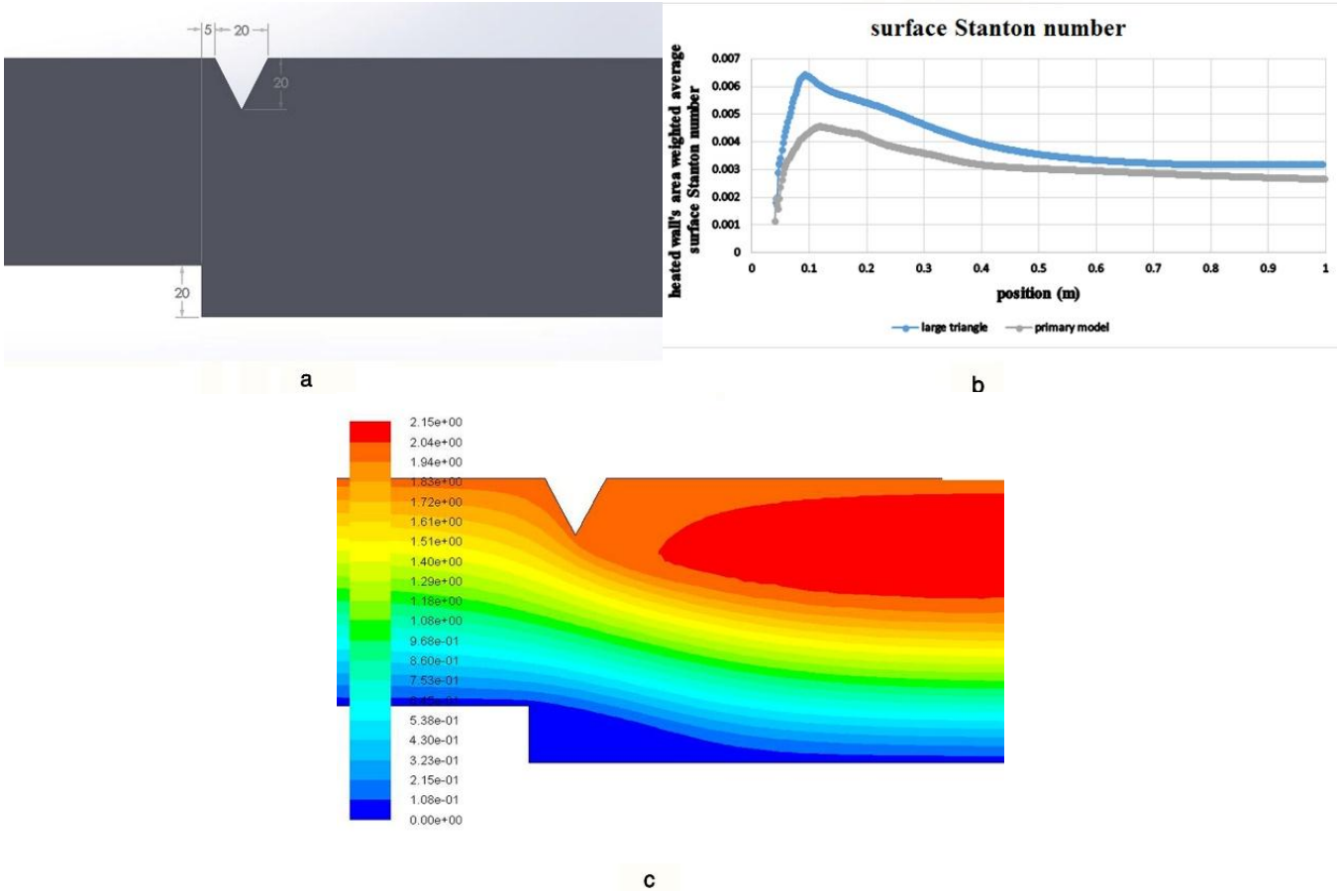

Figure 9. a) Baffle's shape and position (mm), b) Surface Stanton number, c) Stream function

c) Small square

Fifth studied model is a square with side length of 0.01 m and same 0.005 m horizontal distance from the step, discretized with the same meshing mode and boundary conditions as shown in figure 10. Small square showed 2.3435% rise for heated wall's area weighted average Stanton number and 16.553% more pressure drop, so B.C.R should be 0.1416. Obstacle's shape and position, heated wall surface Stanton number and stream function are depicted in figure 10, same as previous cases.

This one acts like previous small size baffles and affects separating and reattached region, not downstream flow. Vortices are fortified and maximum Stanton number is increased, making heat transfer process improved. It should also be noticed that this case has lower pressure loss.

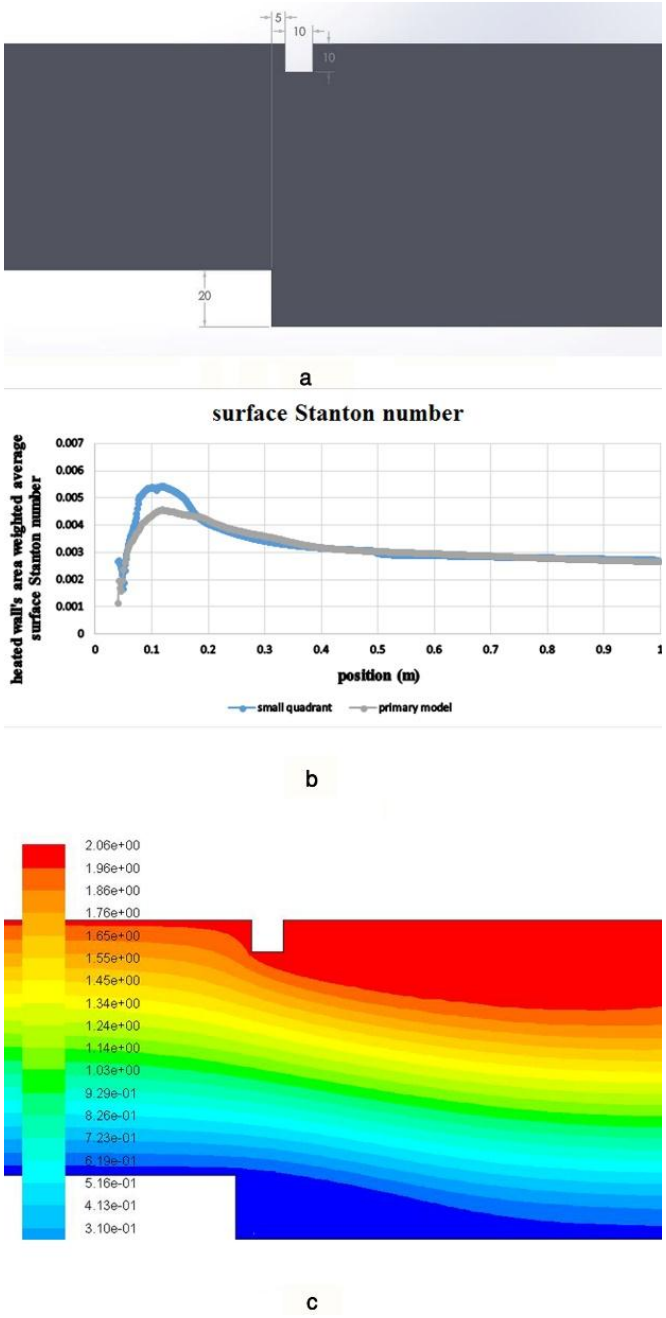

Figure 10. a) Baffle's shape and position (mm), b) Surface Stanton number, c) Stream function

d) Large square

Final model to be investigated is the larger square with 0.02 m side length and same position, domain mesh and boundary conditions are exactly same as all previous baffles. Solving computational domain proves the growth in heated wall's area weighted average surface Stanton number to be 24.916% and its pressure loss to have 48.8405% more, resulting benefit-cost ratio to be 0.4932. Once more, its shape and position, heated wall surface Stanton number compared with primary case and stream function are depicted in figure 11. Larger square apparently affects heat transfer process more profoundly and makes both maximum Stanton number and area weighted average surface Stanton number improve in comparison with Small square. Just like other large baffles, not only does the large square affect separated and reattached region, but it also modifies the downstream flow and consequently, improves both maximum and averaged Stanton number. It makes more intense changes to the flow regime, results in more agitation and increases convection heat transfer coefficient. Noticeable pressure loss is again a weak spot for this baffle.

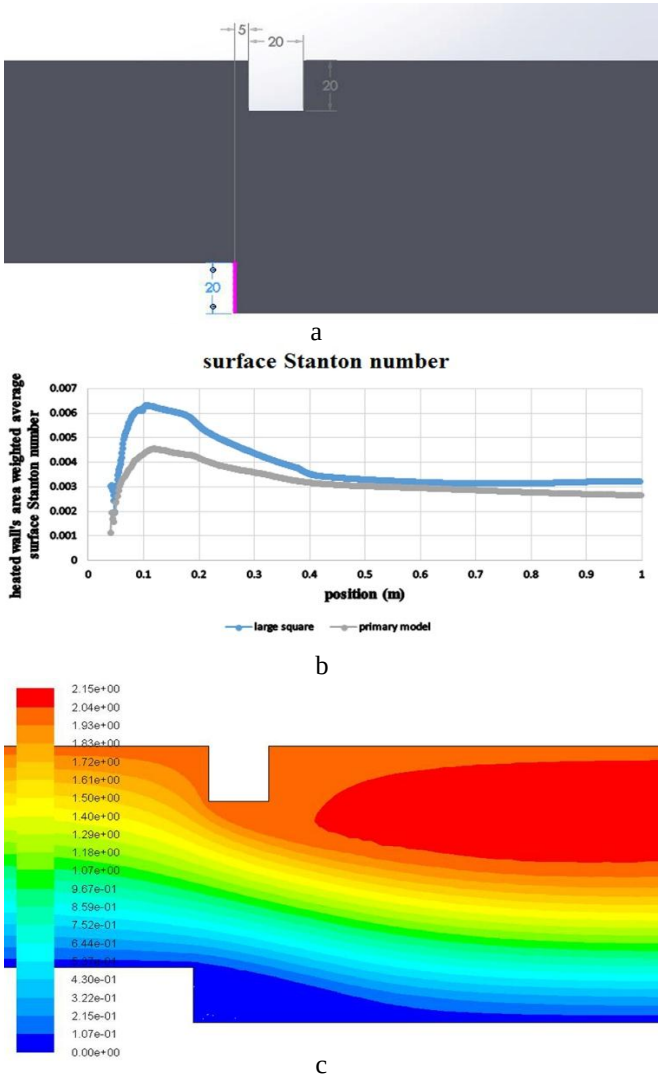

Figure 11. a) Baffle's shape and position (mm), b) Surface Stanton number, c) Stream function

In order to have a more comprehensive understanding of how these obstacles affect the heat transfer phenomenon, all of the aforementioned cases are compared in figure 12. Even though the heated wall's area weighted average Stanton number would be improved by adding small baffles ,it could be increased even more by using the large baffles. In addition,

maximum Stantun number ocuures at about 0.005 m closer to the step while using different shapes of small baffles. This number is about 0.01 m in large baffles. Another point to be considered is the effects of vortex generators on increasing Stantun number away from the step. As the distance from the step increases, the effects of the small baffles become negligible. On the contrary, the large baffles affect further and increase the Stantun number in comparison with previous cases. Finally, it is clear that primary recirculation zone plays a decisive role in heat transfer. In other words, adding obstacles would enlarge the recirculation zone and the larger recirculation zone, the higher Stantun number would be achieved.

Comparing previous results reveals the best condition to be large isosceles triangle with highest benefit-cost ratio. Although this model holds highest increase for heated wall's area weighted average Stanton number, small isosceles triangles showed minimum raise in pressure drop. So, large isosceles triangle has the best performance and will be the basic model for investigating optimum position as shown in figure 12.

B. Baffle's position

After determining the most appropriate shape and size of the baffle, its best location is going to be probed. Like previous section, the ratio of increasing heated wall's area weighted average Stanton number by rising pressure loss that has been defined as benefit–cost ratio (equation 1) is critical criterion for determining best location. Different positions are set and flow field has been solved for each one. Figure 13 illustrates these locations and results for each case.

Holding baffle near the step evinces venture effect and increases velocity, resulting in more agitated vortices which would cause better forced convection heat transfer. Moving baffle along with channel does decrease pressure loss, but not as much as it reduces Stanton number. It also moves the position of region which maximum Stanton number occurs in. Overall, as depicted in figure 13, increasing large isosceles triangle's distance from step has negative effects on B.C.R, although a slight rising occurs at distance of 0.05 m, it is still less than first position. So, overall behavior is negative and the first case (0.005 m distance from the step) is yet the best status.

C. Effects of Reynolds number

After determining the best shape, its size and location, the effects of Reynolds number on benefit-cost ratio would be investigated. Experimental investigation done by Yoshikawa et al. [22] which was chosen as primary form for this research is done at velocity of 20 m/s. Since pressure loss and Stanton number are both functions of air velocity, their values are expected to vary significantly in comparison with experimental investigation and it is not correct to be compared with, so a minimum velocity (3 m/s) is exerted on model with optimum baffle and has been set as primary form for this section. So, all comparisons would be made based on this velocity. Setting same boundary conditions and holding mesh identical, then resolving the flow field again and again with different velocities would reveal the effects of Reynolds number on benefit-cost ratio. These results are depicted in figure 13. Raising Reynolds number would lead to a more turbulent flow, thus better convection heat transfer is anticipated. It increases maximum Stanton number and also moves the point where it happens along the channel. These are caused by higher fluid velocities on agitating flow regime and effects on separating and reattaching region and generated vortices. As shown in figure 14, increasing air velocity would cause area weighted average surface Stanton number of heated wall to rise, but not as sharp as rising pressure loss. This will cause Reynolds number to have adverse effect on benefit-cost ratio.

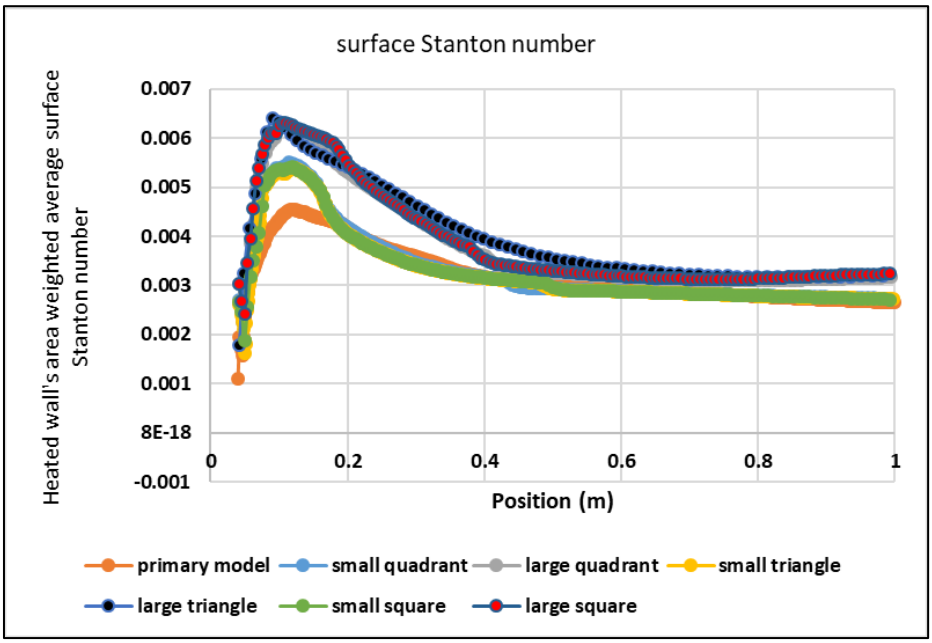

Figure 12. Performance comparison for different baffles

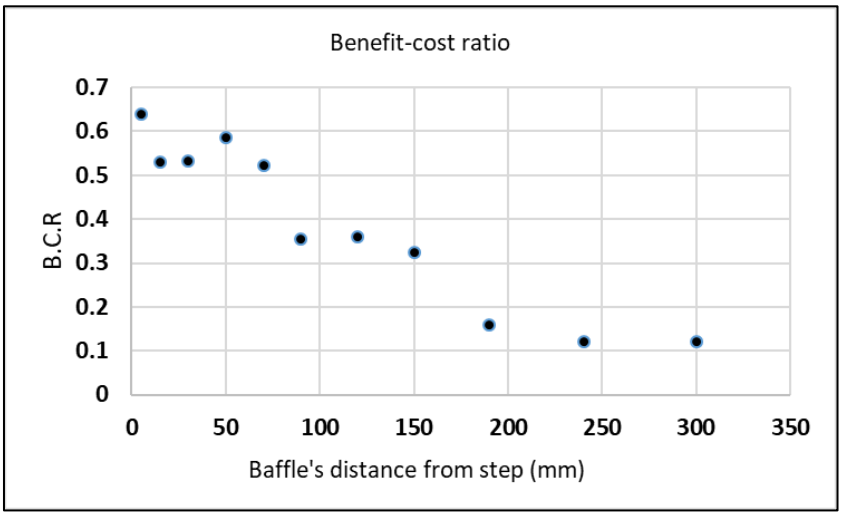

Figure 13. Effects of varying isosceles triangle baffle's position

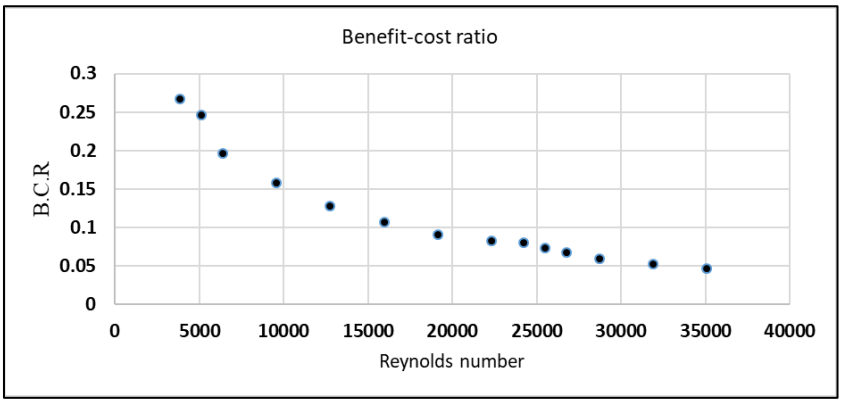

Figure 14. Effect of Reynolds number on B.C.R

IV. CONCLUSION

In order to improve turbulent heat, transfer in separated and reattached flow regions downstream of a downward-facing step, three forms of baffles with quadrant, isosceles triangle and square shape, each one in small (0.01 m) and large (0.02 m) sizes were proposed at a presumed location of 0.005 m distance from the step. All of these obstacles improve turbulent heat transfer by making stream more agitated especially downstream of channel. They also affect the pressure loss and increase it. In order to have a thorough and comprehensive comparison, the ratio of increasing area weighted average surface Stanton number of heated wall by increasing in pressure loss in comparison with primary model was introduced as benefit-cost ratio (B.C.R) and has been set as main criterion. According to B.C.R, large isosceles triangle had best performance among other proposed models. Next step of this research focused on best location of this baffle. So, same baffle was moved along channel and its behavior was detected. Increasing distance of obstacle from step had adverse effect on benefit-cost ratio and best performance was already achieved close to step. With having best shape, size and location of optimum baffle, effect of Reynolds number was investigated and its adverse effect was revealed. So, higher air velocity leads to lower B.C.R.

NOMENCLATURE

ΔP_{int}	Pressure loss of flow through channel without baffle
St_{int}	Heated wall's area weighted average surface Stanton number of channel without baffle
ΔP_{baf}	Pressure loss of flow through channel after adding baffle
St_{baf}	Heated wall's area weighted average surface Stanton number of channel after adding baffle
B.C.R	Benefit-cost ratio
X_t	Channel length
W_2	Total height
W_1	Entrance height
H	Step height
X_E	Step length
q_w	Heat transfer rate
U_{ref}	Free stream velocity

K	Turbulent energy
C1ε, C2ε, C3ε, σk, σε	Model constants
C*p*	Specific heat
Nu	Nusselt number
P	Pressure
Pr	Prandtl number
Re	Reynolds number
St	Stanton number
T	Temperature
u, *v*	Axial velocity
X, *y*	Cartesian coordinates
ρ	Air density
ε	Turbulent dissipation
μ	Dynamic viscosity
μ_t	Turbulent viscosity

REFERENCES

[1] Kumar, S., & Vengadesan, S. (2018). Control of separated fluid flow and heat transfer characteristics over a backward facing step. Numerical Heat Transfer, Part A: Applications, 73(6), 366-384.

[2] Chen, L., Asai, K., Nonomura, T., Xi, G., & Liu, T. (2018). A Review of Backward-Facing Step (BFS) Flow Mechanisms, Heat Transfer and Control. Thermal Science and Engineering Progress.

[3] Atashafrooz, M. (2018). Effects of Ag-water nanofluid on hydrodynamics and thermal behaviors of three-dimensional separated step flow. Alexandria Engineering Journal.

[4] Xu, J., Zou, S., Inaoka, K., & Xi, G. (2017). Effect of Reynolds number on flow and heat transfer in incompressible forced convection over a 3D backward-facing step. International Journal of Refrigeration, 79, 164-175.

[5] Kumar, S., & Vengadesan, S. (2019). The effect of fin oscillation in heat transfer enhancement in separated flow over a backward facing step. International Journal of Heat and Mass Transfer, 128, 954-963.

[6] Tsay, Y. L., Chang, T. S., & Cheng, J. C. (2005). Heat transfer enhancement of backward-facing step flow in a channel by using baffle installation on the channel wall. Acta mechanica, 174(1-2), 63-76.

[7] Heshmati, A., Mohammed, H. A., & Darus, A. N. (2014). Mixed convection heat transfer of nanofluids over backward facing step having a slotted baffle. Applied Mathematics and Computation, 240, 368-386

[8] Nie, J. H., Chen, Y. T., & Hsieh, H. T. (2009). Effects of a baffle on separated convection flow adjacent to backward-facing step. International Journal of Thermal Sciences, 48(3), 618-625.

[9] Abrous, A., & Emery, A. (1996). Benchmark computational results for turbulent backward-facing step flow with heat transfer. Retrieved from

[10] Avancha, R. V., & Pletcher, R. H. (2002). Large eddy simulation of the turbulent flow past a backward-facing step with heat transfer and property variations. International Journal of Heat and Fluid Flow, 23(5), 601-614.

[11] Barbosa-Saldaña, J. G., & Anand, N. (2007). Flow over a three-dimensional horizontal forward-facing step. Numerical Heat Transfer, Part A: Applications, 53(1), 1-17.

[12] Feng, K., LIU, Y.-z., CHEN, H.-p., & Hide, S. K. (2007). Simultaneous flow visualization and wall-pressure measurement of the turbulent separated and reattaching flow over a backward-facing step. Journal of Hydrodynamics, Ser. B, 19(2), 180-187.

[13] Iwai, H., Nakabe, K., & Suzuki, K. (2000). Flow and heat transfer characteristics of backward-facing step laminar flow in a rectangular duct. International Journal of Heat and Mass Transfer, 43(3), 457-471.

[14] Labbé, O., Sagaut, P., & Montreuil, E. (2002). Large-eddy simulation of heat transfer over a backward-facing step. Numerical Heat Transfer: Part A: Applications, 42(1-2), 73-90.

[15] Nie, J., & Armaly, B. F. (2002). Three-dimensional convective flow adjacent to backward-facing step-effects of step height. International Journal of Heat and Mass Transfer, 45(12), 2431-2438.

[16] Saldana, J., Anand, N., & Sarin, V. (2005). Numerical simulation of mixed convective flow over a three-dimensional horizontal backward facing step. Journal of heat transfer, 127(9), 1027-1036.

[17] Selimefendigil, F., & Öztop, H. F. (2013). Numerical analysis of laminar pulsating flow at a backward facing step with an upper wall mounted adiabatic thin fin. Computers & Fluids, 88, 93-107.

[18] Selimefendigil, F., & Öztop, H. F. (2014). Effect of a rotating cylinder in forced convection of ferrofluid over a backward facing step. International Journal of Heat and Mass Transfer, 71, 142-148.

[19] Togun, H., Abdulrazzaq, T., Kazi, S., Badarudin, A., & Ariffin, M. (2013). Heat transfer to laminar flow over a double backward-facing step. Int. J. Mech. Ind. Sci. Eng, 80, 971-977.

[20] Vogel, J., & Eaton, J. (1985). Combined heat transfer and fluid dynamic measurements downstream of a backward-facing step. Journal of heat transfer, 107(4), 922-929.

[21] Wang, B., Zhang, H., & Wang, X. (2006). Large eddy simulation of particle response to turbulence along its trajectory in a backward-facing step turbulent flow. International Journal of Heat and Mass Transfer, 49(1), 415-420.

[22] Yoshikawa, H., Suga, T., & Ota, T. (2005). Turbulent Heat Transfer Around a Downward-Facing Step—Effects of Step Height. Paper presented at the 6th World Conference on Experimental Heat Transfer, Fluid Mechanics and Thermodynamics, Miyagi, Japan.

[23] Öztop, H. F. (2006). Turbulence forced convection heat transfer over double forward facing step flow. International communications in heat and mass transfer, 33(4), 508-517.

How to Cite this Article:

Mohammadi, M., Madanshenas, S., Oreijah, M. & Mohamed, M. H. (2019) Numerical Investigation of Improving Turbulent Heat Transfer in the Separated and Reattached Flow Regions Downstream of a Downward-Facing Step Using Vortex Generators. International Journal of Science and Engineering Investigations (IJSEI), 8(92), 45-55. http://www.ijsei.com/papers/ijsei-89219-05.pdf